# Localization of the Trigger Factor Binding Site on the Ribosomal 50S Subunit

**ARTICLE** *in* JOURNAL OF MOLECULAR BIOLOGY · MARCH 2003

Impact Factor: 4.33 · DOI: 10.1016/S0022-2836(02)01436-5 · Source: PubMed

doi:10.1016/S0022-2836(02)01436-5 J. Mol. Biol. (2003) 326, 887–897

JMB

Available online at www.sciencedirect.com

SCIENCE DIRECT®

# Localization of the Trigger Factor Binding Site on the Ribosomal 50 S Subunit

**Gregor Blaha[1,2], Daniel N. Wilson[1], Gerlind Stoller[3], Gunter Fischer[3] Regine Willumeit[2] and Knud H. Nierhaus[1]***

[1]*Max-Planck-Institut für Molekulare Genetik AG Ribosomen, Ihnestraße 73 D-14195 Berlin, Germany*

[2]*GKSS Forschungszentrum Geesthacht GmbH, Institut für Werkstofforschung WFS Max-Planck-Straße, D-21502 Geesthacht, Germany*

[3]*Max-Planck Forschungsstelle für Enzymologie der Proteinfaltung Weinbergweg 22 D-06120 Halle/S, Germany*

**Corresponding author*

In *Escherichia coli*, protein folding is undertaken by three distinct sets of chaperones, the DnaK-DnaJ and GroEL-GroES systems and the trigger factor (TF). TF has been proposed to be the first chaperone to interact with the nascent polypeptide chain as it emerges from the tunnel of the 70 S ribosome and thus probably plays an important role in co-translational protein folding. We have made complexes with deuterated ribosomes (50 S subunits and 70 S ribosomes) and protated TF and determined the TF binding site on the respective complexes using the neutron scattering technique of spin-contrast variation. Our data suggest that the TF binds in the form of a homodimer. On both the 50 S subunit and the 70 S ribosome, the TF position is in proximity to the tunnel exit site, near ribosomal proteins L23 and L29, located on the back of the 50 S subunit. The positions deviate from one another, such that the position on the 70 S ribosome is located slightly further from the tunnel than that determined for the 50 S subunit alone. Nevertheless, from both determined positions interaction between TF and a short nascent chain of 57 amino acid residues would be plausible, compatible with a role for TF participation in co-translational protein folding.



*Keywords:* trigger factor; ribosome; 50 S subunit; neutron scattering; spin-contrast variation

## Introduction

Folding of newly synthesized polypeptides within the cytosol of bacteria, such as *Escherichia coli*, utilizes three distinct sets of chaperones, the DnaK and GroEL systems and the trigger factor (TF). Unlike the DnaK and GroEL systems, which have been under intensive study since the late 1970s,[1–3] the importance of TF has only recently become apparent.

TF was originally assigned the status of a secretion-specific chaperone;[4–6] a proposal that was later rejected when cells depleted for TF did not display pleiotropic secretion defects.[7] Subsequently, TF was shown to have a broad binding specificity, being found interacting with both cytoplasmic and secretory nascent chains within translating ribosome complexes.[8–10]

*E. coli* TF is composed of 432 residues, has a mass of 45 kDa and exhibits a modular structure.[11] Sequence analysis identified TF as a member of the FK506 binding protein chaperone family and suggested that the central portion of TF possess peptidyl-prolyl *cis/trans* isomerase (PPIase) activity.[12,13] Limited proteolysis defined a minimal PPIase domain of TF, constituting residues 132–251, which was able to refold protein.[13,14] The association of TF with ribosomes[15] was shown to be essential for efficient cross-linking with the nascent chain.[8,9] Although the N-terminal domain of TF, consisting of residues 3–118, was shown to be sufficient for ribosome binding and competed efficiently for binding with the full-length protein,[16] evidence suggests that the central and C-terminal domains strengthen this interaction further: complexes formed between TF and translating

Present address: G. Blaha, Department of Molecular Biophysics and Biochemistry, Yale University, 266 Whitney Avenue/Bass 415, P.O. Box 208114, New Haven, CT 06520-8114, USA.

Abbreviations used: Cr(V)-EHBA, sodium bis(2-ethyl-2-hydroxybutyrato)oxo-chromate(V) monohydrate; superscript D (as in $^{D}$50 S), deuterated 50 S subunit; TF, trigger factor; PPIase, peptidyl-prolyl *cis/trans* isomerase; aa, amino acid residue(s); DPN, dynamic nuclear polarization.

E-mail address of the corresponding author: nierhaus@molgen.mpg.de

0022-2836/03/$ - see front matter 

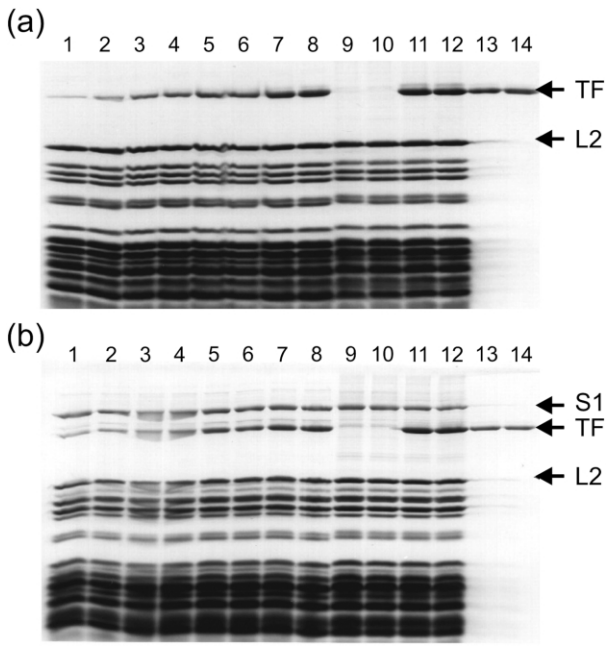


**Figure 1**. Quantification of trigger factor complexes. SDS-PAGE analyses of (a) $^{D}$50 S-TF and (b) $^{D}$70 S-TF complexes. Duplicate loadings of 1 $A_{260}$ for each TF complex (lanes 11 and 12) were compared with standard loadings of trigger factor protein (lanes 13 and 14 are 36 pmol in (a) and 24 pmol in (b)). Lanes 1 to 10, as a control 1 $A_{260}$ of 50 S subunits or 70 S ribosomes were mixed with different amounts of TF and loaded onto the gel (molar ratios of TF/ribosomes of lanes 1–8 were 0.2, 0.4, 0.6, 0.8, 1.0, 1.2, 1.4, 1.6, in (a) for $^{D}$50 S subunit and in (b) for $^{D}$70 S ribosome; Lanes 9 and 10 were in the absence of TF). The positions of the trigger factor (TF) and ribosomal protein S1 (only in 70 S ribosomes) are arrowed, as is ribosomal protein L2, with which the ribosome loadings were normalized between lanes. Note: the complexes analyzed in lanes 11 and 12 were created using a 15-fold excess of TF over ribosomes.

ribosomes were resistant to high-salt wash treatment, in contrast to complexes formed with non-translating ribosomes, which were not. Furthermore, addition of puromycin to the translating ribosome–TF complexes, resulting in the release of the nascent chain from the ribosome, or deletion of the C-terminal domain, thought to interact with the nascent chain, resulted in TF complexes susceptible to high-salt wash treatment.[16] The affinity of TF for peptides in solution is low, supporting the notion that ribosome binding plays an important part in enhancing the TF–peptide interaction.[17]

Surprisingly, binding to unfolded proteins was not restricted to substrates that contain proline residues, even though proline residues are the substrate for the PPIase activity. A recent study using 13-meric peptide libraries identified a fairly degenerative TF binding motif that determines substrate specificity and predicted a binding pocket in the PPIase domain, on the basis of homology modeling, that interacts directly with this binding motif.[17] TF itself has been shown to exhibit a molecular chaperone-like function.[18–21] Although the chaperone-like function and the PPIase activity may both be attributed to the same binding pocket on the TF,[17] PPIase activity is not required for efficient refolding activity.[22] Furthermore, TF has been shown to cooperate with other chaperone systems, such as GroEL-GroES.[23,24] This is exemplified by the interesting dynamic that exists between TF and DnaK. Deletion of the TF gene, *tig*, or the *DnaK* gene is tolerated by the cell and does not result in any folding defects at permissive temperatures,[19,25–27] but inactivation of both genes is lethal.[2,27,28] This obvious compensatory relationship between the two factors is supported by the observation that, in cells deficient for TF, there is a two- to threefold higher association of DnaK with the nascent polypeptide.[27,28] The importance of TF is further emphasized by the retention of the *tig* gene in *Mycoplasma* species, despite the loss of all other PPIases.[29] Furthermore, that TF interacts with all forms of nascent chain-ribosome complexes, even when the nascent chain is of only 57 aa in length, and that the tunnel of the 50 S ribosomal subunit protects up to 40 aa, implicates TF as the first chaperone to interact with the nascent chain. This led to the suggestion that TF binds to the ribosome near the exit site and assists with co-translational folding.

We have determined the TF binding site on the 50 S subunit and on the 70 S ribosome by means of the neutron scattering method of spin-contrast variation. Of all the small-angle scattering methods, spin-contrast variation produces the best signal-to-noise ratio and has been successfully applied to the ribosome.[30–36] Our results suggest that TF binds the ribosome in the form of a homodimer. The close proximity of our determined TF binding site to the tunnel exit site on the 50 S subunit, such that translation of a nascent chain of 57 amino acid residues would be of sufficient length to enable contact with the TF, is compatible with a role for TF in co-translational folding.

## Results

### Preparation of trigger factor-ribosome complexes

Purified deuterated 50 S subunits and 70 S ribosomes ($^{D}$50 S and $^{D}$70 S, respectively) were bound by protated TF protein simply by mixing 50 S subunits or 70 S ribosomes with a 15-fold excess of TF and incubating for 30 minutes at 37 °C (as described in Materials and Methods). Subsequently, the complexes were centrifuged through a 15% (w/v) sucrose gradient to remove unbound trigger factor and the resultant complexes were analyzed by SDS-PAGE. Representative gels for the $^{D}$50 S-TF and $^{D}$70 S-TF complexes are shown (Figure 1, lanes 11 and 12 in (a) for 50 S and (b) for 70 S complexes, respectively). Accurate determination of the stoichiometry of the $^{D}$70 S-TF (or $^{D}$50 S-TF) complexes was possible by comparison

**Table 1.** Preparation and quantitation of $^{D}$50 S-TF and $^{D}$70 S-TF complexes for spin contrast variation

| | TF excess | Ribosome or subunit recovery (%) | Rotor type and centrifugation conditions | Sucrose gradient (max. %) | Occupancy of TF on ribosome |
|---|---|---|---|---|---|
| $^{D}$50 S | 15 | 63 | SW40, 21 hours, 22,000 rpm | 15 | 1.71 |
| $^{D}$70 S | 15 | 72 | SW40, 21 hours, 22,000 rpm | 15 | 1.83[a] |
| $^{D}$50 S | 10 | 66 | 70 Ti, 6 hours, 26,000 rpm | 15 | 1.36[a] |
| $^{D}$70 S | 10 | 72 | 70 Ti, 6 hours, 26,000 rpm | 15 | 0.98 |
| $^{D}$50 S | 8 | 75 | 70 Ti, 10.5 hours, 26,000 rpm | 20 | 1.56 |

[a] TF complexes chosen for neutron scattering analyses.

with lanes 1 to 8, where a mixture of 70 S ribosomes (or 50 S subunits) with increasing amounts of TF were applied (molar ratios TF:ribosomes = 0.2 to 1.6).

All complexes were quantified by densitometry and the normalized values are presented in Table 1. The stoichiometry of TF binding to 70 S and 50 S using a 15-fold excess of TF was much higher than expected. The expectation was based on the binding values obtained when TF was bound to protiated 50 S subunits or 70 S ribosomes (under identical conditions). In this situation lower TF binding values were obtained, although they were almost always above one per particle at higher excess of TF but never exceeded two (data not shown). This suggested that TF has a slightly higher affinity for deuterated ribosomes than protated. Attempts were made to reduce TF binding by increasing the stringency of the complex isolation procedure; namely, by increasing the sucrose viscosity (from 15% to 20%), and reducing the TF excess. The results of these procedures are summarized in Table 1. Stoichiometric TF binding was observed with the $^{D}$70 S ribosomes but not with the $^{D}$50 S subunit. With $^{D}$50 S subunits, binding was always between 1.0 and 2.0, despite a combination of decreasing TF excess and increasing both the spin time and the sucrose viscosity. This suggested that TF might bind in the form of a dimer or has two stable binding sites on the ribosome. With a binding ratio for the $^{D}$50 S-TF complex of 1.36, the occupancy (ligands/ribosome) would be approximately 0.7, if a single stable binding site for a TF dimer existed. Likewise, the $^{D}$70 S-TF complex with the highest binding ratio of 1.83 would have an occupancy of around 0.9 in the case of a TF dimer.

**Table 2.** Chemical composition of the samples $^{D}$50 S-TF and $^{D}$70 S-TF prepared for spin-contrast variation (all weights in mg)

| Sample | $^{D}$50 S-TF | $^{D}$70 S-TF |
|---|---|---|
| Concentration ($A_{260}$/ml) | 455 | 360 |
| Ribosomes | 12.93 | 10.93 |
| $^{2}H_2O$ | 798.29 | 811.97 |
| $H_2O$ | 1.60 | 1.63 |
| [$^{2}$H]Glycerol | 980.49 | 975.06 |
| [H]Glycerol | 12.91 | 12.84 |
| Cr(V)-EHBA | 16.40 | 17.00 |
| Imidazole, $MgCl_2$, KCl | 23.67 | 8.36 |

## Localization of trigger factor on the 50 S subunit and 70 S ribosome: methodology

The selected complexes, $^{D}$50 S-TF and $^{D}$70 S-TF, used for nuclear spin-contrast variation were treated as described in Materials and Methods and the chemical composition of these samples is summarized in Table 2. The scattering spectra were measured with the SANS1 instrument at the GKSS research center. Spectra were taken for the unpolarized target and with either parallel or antiparallel aligned proton spins, relative to the spins of the incoming neutrons. The collected data were processed according to the standard corrections and deconvoluted into the three basic scattering functions $U(q)^2$, Re$[U(q)V(q)]$ and $V(q)^2$. These scattering functions were fitted using basic scattering functions obtained from an electron microscopy structure of the 50 S subunits[37] and 70 S ribosomes,[38] onto which the position of the TF was determined. In a first step, the radius of gyration $R_G$ and the coordinates of the center of mass of the TF protein were determined. For the calculation of the coordinates, the simplest case scenario of a spherical shape for the TF protein was assumed. The sphere was permitted to shift to any position within the ribosomes and vary in size. In principle, from comparison of the measured $R_G$ with a theoretical $R_G$ value calculated from the mass of the protein, an idea of the overall molecular dimensions of the TF protein can be gained.

## Trigger factor binds to the 50 S subunit in the vicinity of the tunnel exit site

In the absence of a crystal structure for the TF, the assumption was made that TF is a moderately dense (1.35 g/cm$^3$) protein with a spherical morphology within the 50 S subunit, a calculation of the radius of gyration yields a theoretical $R_{G,theo}$ value of 18.7 Å. Our neutron scattering measurement resulted in a radius of gyration $R_{G,50\,S}$ of 30(±3) Å. This difference can best be explained if we assume the TF binds in the form of a dimer with a slightly elongated shape, characterized as a prolate ellipsoid of revolution with an axis ratio of about 2.5. This assumption is in agreement with the observed binding stoichiometry of more than one TF molecule per particle. In this case, a single binding site of the bound TF would be expected.

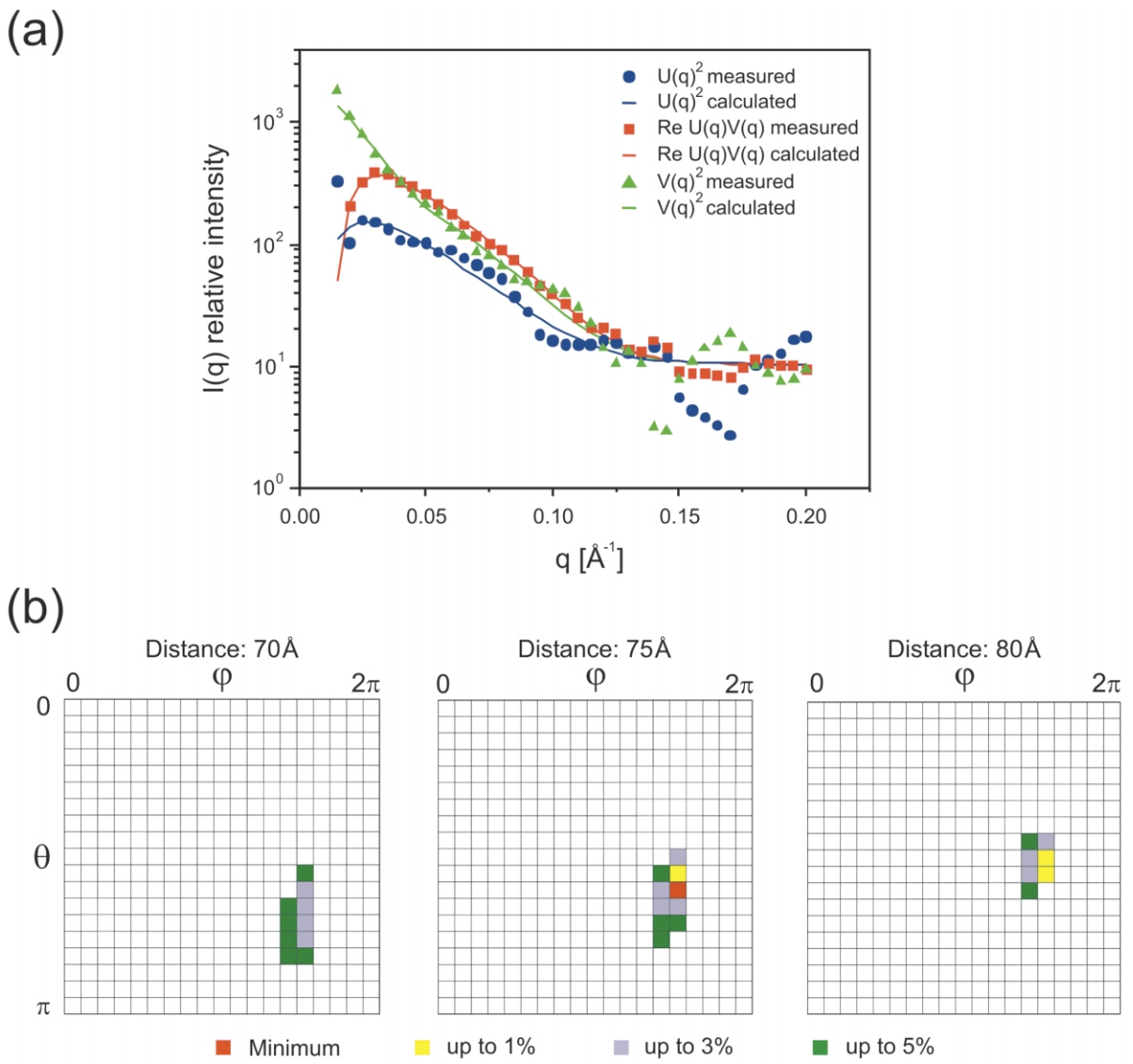


**Figure 2**. Neutron scattering results from the $^{D}$50 S-TF complex. (a) The measured and modeled (calculated) basic scattering functions are shown for the best fit of the data. The scattering function Re[$U(q)V(q)$] was multiplied by (−1) and all three basic scattering functions were increased by a value of 10 for convenience of display. (b) "Minimum maps" displaying the TF position on the 50 S subunit. For each of the three maps, the distance from the center of mass of the 50 S subunit to the TF is given, together with the *R*-values obtained from the fitting procedure. The best *R*-value was 2.524, which represented the minimum (red). Positions with *R*-values up to 5% larger than the minimum located near to the minimum indicate the certainty of the fit.

The position of the center of mass for the TF within the 50 S subunit can be expressed using polar coordinates ($r$, φ and θ). The coordinates of the center of mass of the protated label in either state were varied stepwise over the total volume of the 50 S subunit and its near vicinity during the fitting procedure. The root-mean-square deviation $R$ (see Materials and Methods) of the theoretical and experimental basic scattering functions were calculated and the parameter set with the smallest value of $R$ represents the center of mass of the TF within the ribosome in the state under consideration.

The center of mass for TF was found on the back-side (solvent side) of the 50 S subunit and had an *R*-value of 2.524 (the minimum). The quality of the fit for the three characteristic functions is shown in Figure 2(a). The good correlation between the measured and calculated scattering functions at lower $q$ values (i.e. those less than 0.1) reflects the accurate global assignment of the TF position. The loss of correlation between the measured and calculated data at larger $q$ values (and thus at shorter proton distances within TF) reflects the lack of resolution in assigning the TF "micro-environment" and thus most likely results from the incorrect assumption that the TF protein has a spherical form. The distance $r$ of the TF protein from the center of mass of the 50 S subunit, which is the origin of our coordinate system, was

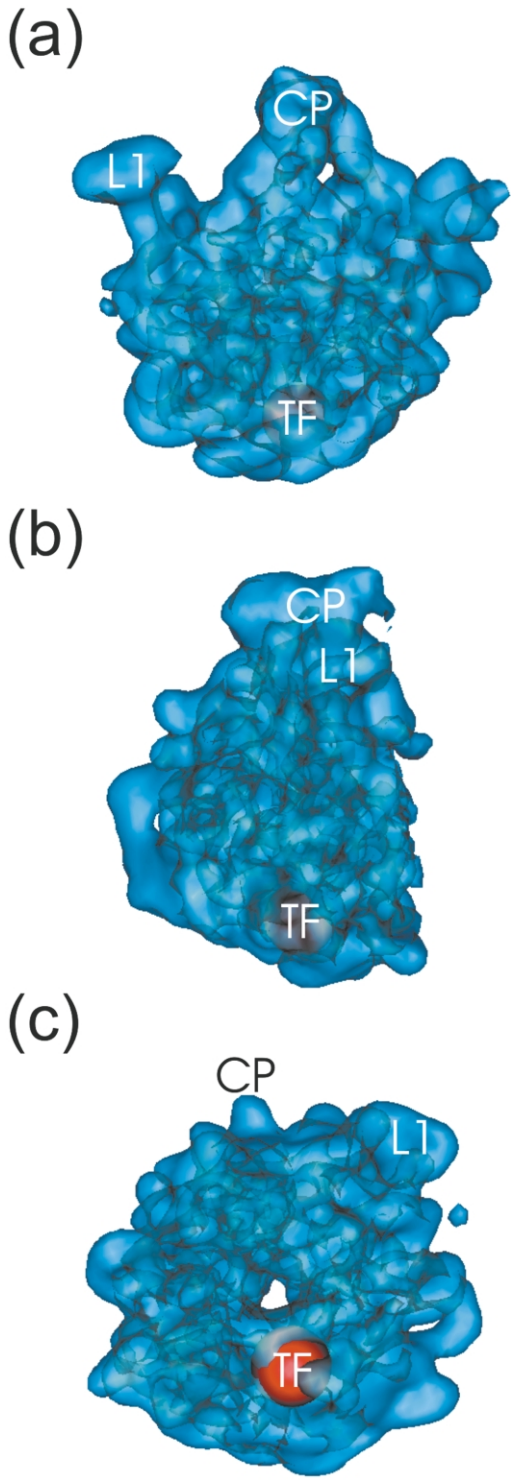


**Figure 3**. Trigger factor position on the 50 S subunit. TF position, represented by a red sphere of radius 20 Å, corresponds with data based on the best *R*-value (minimum at 2.524). The orientation of the 50 S subunit is, from top to bottom, the crown perspective, side-view with L1 to the foreground and bottom view centered on the tunnel. The ribosomal landmarks L1 and CP represent the L1 stalk and the central protuberance, respectively. The ribosome model is from Malhotra and coworkers.[57]

78(±15) Å, while the angle values were $\varphi = 1.74$ rad and $\theta = 4.8$ rad. The position can also be described using Cartesian coordinates $x = 7(\pm 5)$ Å, $y = -76(\pm 15)$ Å and $z = -12(\pm 6)$ Å. The critical fit parameters are the angles $\varphi$ and $\theta$ which cannot be determined unambiguously. To test the stability of the results, i.e. whether there are local minima around the absolute minimum or whether one global minimum exists, all possible combinations of $r/\varphi/\theta$ were calculated and presented in a $\varphi$ *versus* $\theta$ map for distinct $r$ values (Figure 2(b)). Although it was clear that the minimum value determined from this analysis represents a single global minimum, neighboring coordinates also show values within 1% of the minimum. This indicates some degree of shallowness in the minimum, perhaps reflecting non-specific TF binding in neighboring positions to the minimum. The position of TF on the 50 S subunit, as obtained by single-sphere modeling, is shown in Figure 3. This places the TF position 40 Å from the edge of the tunnel exit, when measuring to the center of TF sphere (center of mass for the data set with the minimum *R*-value). The existence of a single global minimum agrees well with a single binding site and together with the $R_G$ value implies the presence of a dimer.

### The trigger factor binding site on the 70 S ribosome

The data for the $^{D}$70 S-TF complex were treated as described in the preceding section for the 50 S subunit. The final results for the data processing with the modeling of a spherical protein are shown for the three basic scattering functions in Figure 4(a). Again a good agreement between calculated and measured curves can be found for medium and small $q$-values while in the larger $q$ regime the description of the measured curves by the theoretical ones is not sufficient. As in the 50 S case, this can be explained by an inappropriate description of the protein by a sphere. This also agrees well with the high radius of gyration, as it was identical with that for TF on the 50 S subunit, $R_{G,70\,S}$ of 30(±3) Å, despite the supposed higher occupancy of the TF on the 70 S than had been obtained for the 50 S. Again this argues for the presence of a dimer with the same overall dimensions as characterized for the 50 S, namely a prolate ellipsoid of revolution with a ratio of the main axis of about 2.5. The center of mass of the TF was 123(±5) Å from the center of mass of the 70 S ribosome, the origin of the coordinate system. A much more defined position for TF on the 70 S ribosome than on the 50 S subunit was determined, in that only one deep minimum was found (Figure 4(b)). With angle values of $\varphi = 1.65$ rad and $\theta = 2.75$ rad ($x = -114(\pm 5)$ Å, $y = 45(\pm 5)$ Å and $z = -4(\pm 3)$ Å), the position of the TF on the 70 S ribosome locates to the back side of the 50 S subunit, slightly further from the tunnel exit site than the position found on the 50 S subunit alone (Figure 5).

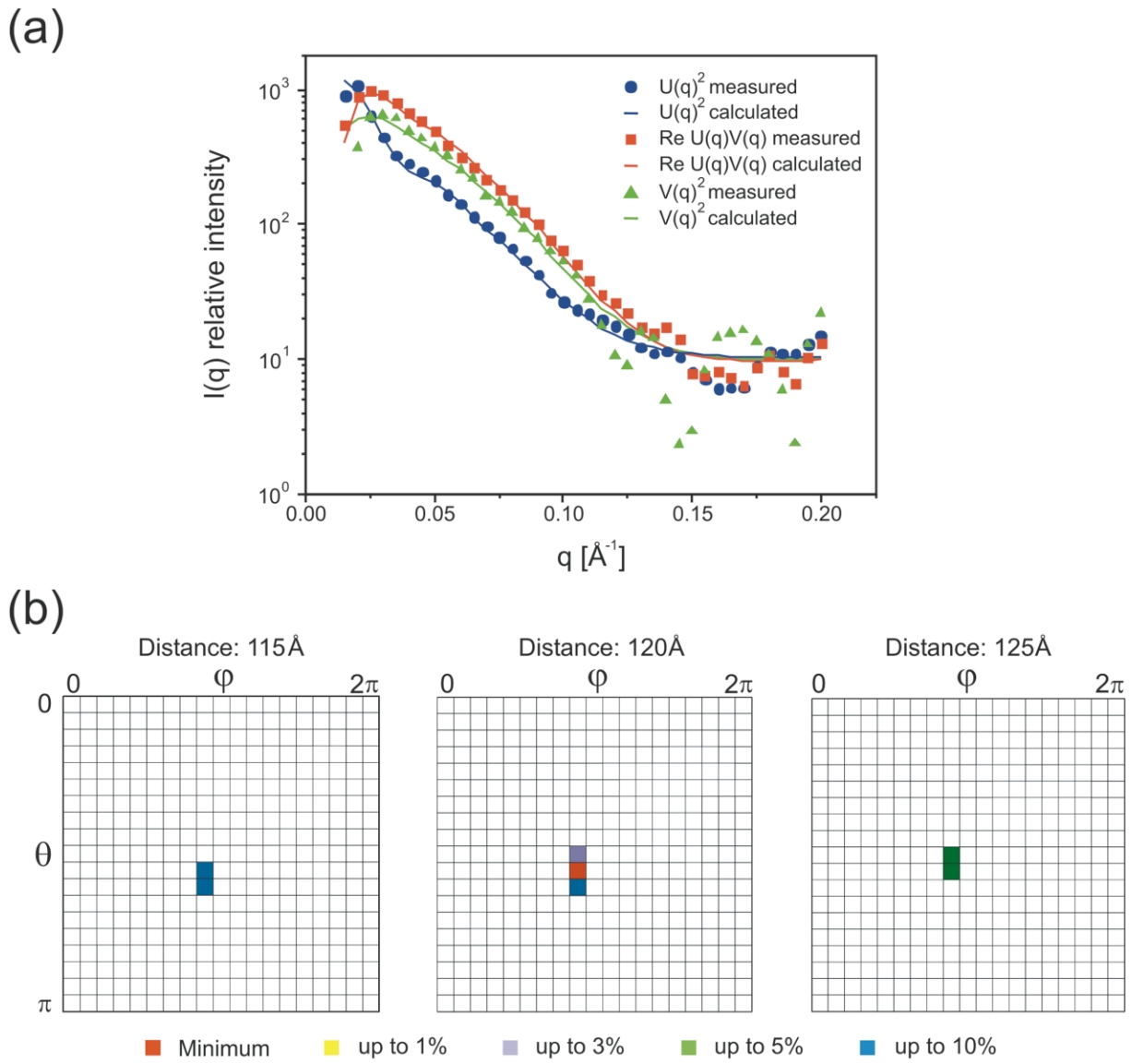


**Figure 4**. Neutron scattering results from the $^{D}$70 S-TF complex. (a) The basic scattering functions are shown with the lines representing the optimal fit for each data set. The scattering function Re[$U(q)V(q)$] was multiplied by (−1) and all three basic scattering functions were increased by a value of 10 for convenience of display. (b) Minimum maps displaying the TF position on the 70 S ribosome. For each of the three maps, the distance from the center of mass of the 70 S ribosome to the TF is given, together with the *R*-values obtained from the fitting procedure. The best *R*-value was 2.754, which represents the minimum (red). Positions with *R*-values up to 10% larger than the minimum located near to the minimum indicate the certainty of the fit.

## Discussion

TF may be the first chaperone to bind to the nascent polypeptide chain as it emerges from the ribosome. The N-terminal domain of TF is shown to be sufficient for ribosome binding although interaction with the nascent chain, *via* the central domain of the TF, strengthens this interaction.[16] That TF interacts with the nascent chain[8–10] and has been shown to bind specifically to the 50 S subunit[15] suggested that the binding site of TF should be located near to the exit site of the ribosome tunnel on the back of the 50 S subunit.

We have determined the TF binding site on the 50 S subunit, alone and within the 70 S ribosome, in the absence of a nascent chain. On the 50 S subunit alone, the center of mass for TF was located 40 Å from the tunnel exit site, whereas on the 70 S ribosome the position was another 20 Å further from the exit site. This difference between the two positions may result from conformational changes that the 50 S subunit undergoes during the association with the small subunit to form a 70 S ribosome. Such a conformational change cannot be traced by activation energy measurements, but rather by functional studies (for discussion see Blaha *et al.* [39]). In principle, the position of TF on the 50 S subunit should better represent a single binding site, as the binding ratio of TF/50 S was 1.36:1 as compared with 1.83:1 with the 70 S

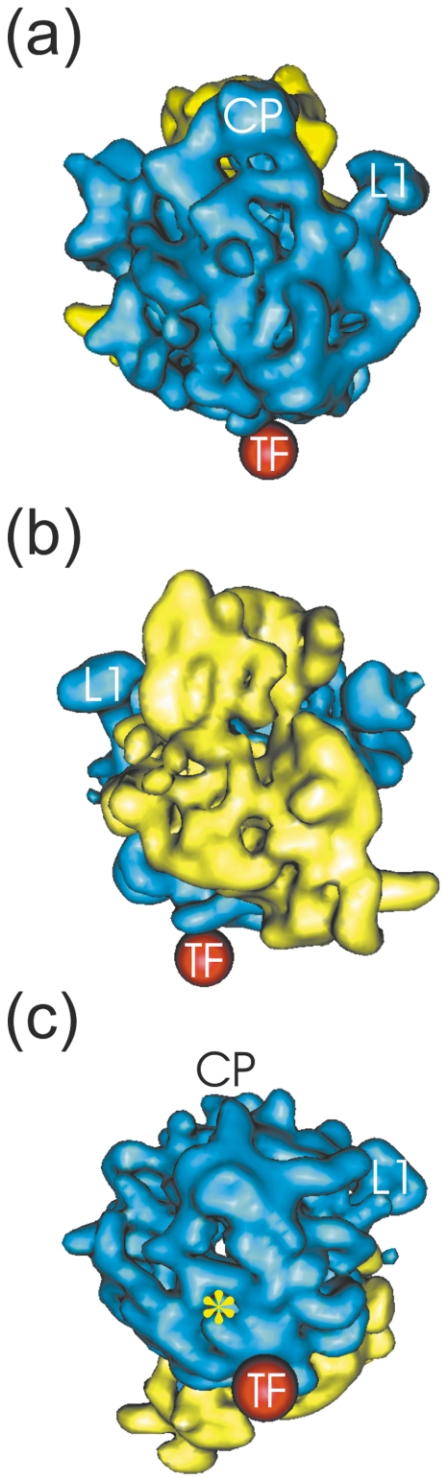


**Figure 5**. Trigger factor binding position on the 70 S ribosome. The TF position based on the best *R*-value of 2.754 is represented by a red sphere of radius 20 Å. The orientation of the 70 S ribosome is, from top to bottom, with 50 S (blue) in the foreground, with 30 S (yellow) in the foreground and bottom view with L1 in the top right-hand corner. The ribosomal landmarks L1 and CP represent the L1 stalk and the central protuberance, respectively. The subunits of the ribosome model[57] were identified by cutting the 70 S ribosome through the bridges that connect the 50 S and 30 S subunits The yellow asterisk ( ∗ ) in the bottom view of the 70 S ribosome indicates the TF binding position on the 50 S subunit with the highest *R*-value.

ribosome. Surprisingly, on the 70 S ribosome we detected only a single minimum, instead of the dual minimums reflecting the two binding sites that might have been expected. Furthermore, the localization of the center of mass for the TF on the 70 S ribosome was determined with more certainty than that on the 50 S, i.e. the minimum was deeper. Our data determine the center of mass for the TF protein assuming a spherical shape, so it is inevitable that an elongated shape would distort our data somewhat (as evident by the loss of correlation at larger $q$ values in Figures 2(a) and 4(a)). But in both cases, although recalculation of the data on the basis of an elongated shape may improve the minimum slightly, it is unlikely to affect the determined positions significantly.

However, if we conclude that TF binds to the ribosome in the form of a dimer then the occupancy of the 70 S is over 90%, which correlates better with the single deep minimum. We note that several other lines of evidence suggest that the TF binds to the ribosome in the form of a homodimer: (a) even with large excesses of TF over ribosomes (up to 20-fold), the TF:ribosome ratio never exceeded 2. (b) The binding values observed with complexes could not be reduced significantly even when the stringency of the isolation method was increased (Table 1). (c) The same $R_G$ value of 30(±3) Å was determined for both 50 S subunit and 70 S ribosome complexes, despite significantly different occupancies (1.36 and 1.83, respectively, assuming TF as a monomer). For a TF dimer this $R_G$ value indicates an overall shape best described by a prolate ellipsoid having an axial ratio of 2.5. (d) Although the protated 50 S subunits had a lower affinity for TF, stoichiometries significantly greater than 1.0 were also observed, suggesting that the binding values are not simply artifacts due to the deuteration. (e) In the case of the 70 S complex, the fact that stable binding of 1.83 TF molecules per 70 S ribosome coupled with the finding of a unique single binding site argues strongly in favor of dimerization.

That the TF has been cross-linked to a nascent peptide of only 57 aa would suggest that it binds within the vicinity of the tunnel exit. Assuming the ribosome tunnel protects between 30 aa and 40 aa,[40–42] then 17–27 aa of the 57 aa could potentially have emerged from the tunnel. When in an α-helical conformation, the distance traveled (termed the "rise") by a polypeptide chain is 1.5 Å per amino acid residue, or 3.6 Å when the chain is fully extended. Thus, for a stretch of between 17 aa and 27 aa, this would equate with 25.5–40.5 Å and 59.5–97.2 Å, respectively. We note that the former α-helical conformation for the nascent chain is the more probable,[43,44] which would restrict interaction of the tail of a 57 aa nascent chain to a radius of 25–40 Å from the tunnel exit. This is easily within range to enable interaction between the nascent chain and the TF bound at the position determined on the 50 S subunit. Taking into consideration that the 40 Å distance from the $^{D}$50 S-TF position to the

exit site is measured from the center of mass of the TF (sphere of radius 20 Å), this would suggest that interaction would be theoretically possible at any distance greater than 20 Å. Similarly, the $^{D}$70 S-TF position could make interaction with the nascent chain at any distance greater than 40 Å. Thus, in principle, both TF positions determined could fit the biochemical cross-linking data.

On the basis of the crystal structures of the 50 S subunit at atomic resolution,[45,46] the TF binding site on the 50 S subunit would be expected to be around the universally conserved ribosomal protein L23, located just below the tunnel exit site, and on the 70 S ribosome, shifted towards the neighborhood of ribosomal protein L29. Recently, cross-links from ribosome-bound TF identified both ribosomal proteins L23 and L29 as being close neighbors.[47] L23 specifically was shown to be essential for TF interaction with the ribosome and was proposed to be the chaperone-docking site on the ribosome.[47] The discovery that SRP54 of the signal recognition particle also forms a cross-link with the eukaryotic L23 homologue,[48] suggests that the exit site of the ribosome may play an important role in guiding nascent chains to their appropriate destination.[49]

In conclusion, the positions determined for the TF on the 50 S subunit and the 70 S ribosome support the role of the TF in co-translational folding of nascent polypeptides on the ribosome. The similarity in the general binding position for TF on empty ribosomes (this study) as on translating ribosomes[47] could indicate that TF may bind before the nascent chain has even emerged from the tunnel. It is interesting to note in this respect that TF binding to the ribosome was a prerequisite for association of the TF with the nascent chain.[47]

## Materials and Methods

Fully deuterated cells of *E. coli* strain MRE600rif were purchased from CDN Ltd, Tallinn, Estonia (cdnest@hotmail.com). Purified trigger factor protein was purified as described.[8] All other chemicals including $^{2}H_2O$ and [$^{2}$H]glycerol were purchased from Merck, Darmstadt. Buffer conditions use the following abbreviations: H, Hepes–KOH (pH 7.6 at 0 °C); M, $MgCl_2$; K, KCl; N, $NH_4Cl$; $SH_4$, 2-mercaptoethanol; Im, imidazole–HCl (pH 7.6 at 0 °C); Spd, spermidine, Sp, spermine; the mM final concentration of which is represented by a subscript following the abbreviation, e.g. $M_{20}$ equates with 20 mM $MgCl_2$. Note that all buffer constituents, imidazole, $MgCl_2$ and KCl in the deuterated buffer had been previously lyophilized and dissolved in $^{2}H_2O$ (repeated three times) to ensure removal of exchangeable protons or protated crystal water.

### Preparation of deuterated 50 S subunits and 70 S ribosomes

The preparation of 70 S ribosomes and 50 S subunits from the deuterated *E. coli* cells was essentially undertaken as described.[50,51] Briefly, 50 S subunits were isolated by zonal centrifugation through a 6% to 38% (w/v) sucrose gradient in $H_{20}M_1N_{200}SH_4$ buffer (17 hours at 23,000 rpm in a $T_i$ 15 rotor), the 30 S and 50 S peak fractions were pooled separately, pelleted by ultracentrifugation (20 hours at 100,000*g* in a 45 $T_i$ rotor) and resuspended in $H_{20}M_6K_{30}$ buffer. The 70 S ribosomes were prepared from the re-association of the 30 S and 50 S subunits simply by mixing the respective subunits at a 30 S/50 S stoichiometry of 2:1, under $H_{20}M_{20}K_{30}$ buffer conditions and incubating at 40 °C for 40–60 minutes. The 70 S re-associated ribosomes were separated from subunits by repeating the aforementioned zonal centrifugation procedure.

During the preparation extreme care was taken to prevent ribonuclease contamination. Therefore, only glassware pre-baked at 180 °C for at least two hours, or autoclaved plastic tubes and pipette tips, were used and all procedures were conducted at 4 °C.

### Preparation and quantification of trigger factor–ribosome complexes

With the neutron scattering technique using spin-contrast variation, a sample volume of 600 μl with a concentration of approximately 25 mg/ml is required. To meet this requirement, 500 $A_{260}$ of deuterated ribosomes (or 50 S subunits) were incubated, with varying excesses of trigger factor (see Results), for 30 minutes at 37 °C in a final volume of 3.5 ml in $H_{20}M_6N_{150}SH_4Spd_5Sp_{0.05}$. The trigger factor remaining unbound was separated from the ribosome (or 50 S subunits) bound factor *via* centrifugation through a 13.3 ml 15% (w/v) sucrose cushion for 21 hours at 22,000 rpm as described. Note that the sucrose cushion, centrifugation time, speed and rotor were varied in an attempt to control the stoichiometry of the trigger factor–ribosome complex (see Table 1). In all cases the pellet was re-suspended in 400 μl in $Im_{100}M_{10}K_{100}$ buffer and extensively dialyzed (four times for 30 minutes in 50 ml) against the same buffer to remove exchangeable protons from the sample. Insoluble or non-dissolved particles were removed by centrifugation in a microfuge for five minutes at 10,000 rpm (4 °C). Before snap-freezing in liquid nitrogen, a 25 μl aliquot was removed in order to quantify the stoichiometry of the ribosome–TF complexes.

A sample of 1 $A_{260}$ of ribosome–TF complex was separated on a 12% (w/v) polyacrylamide gel. To enable accurate quantification, 1 $A_{260}$ of 70 S ribosomes (or 50 S subunits), together with varying amounts of TF (ranging from 0.2–1.6 × the ribosome concentration), were loaded into neighboring lanes of the gel. Gels were run for two hours at 150 V and then stained with Coomassie blue. Protein bands were measured densitometrically and quantified using ImageQuant (Molecular Dynamics). Quantification of ribosome (or 50 S)-bound trigger factor was determined by comparison of band intensities with the neighboring TF standards. A comparison of the band for ribosomal protein L2 between standard and complex lanes was used to determine the actual amount of ribosome present in the complexes. This value was then used to determine the stoichiometry of the TF–ribosome complexes.

In order to perform nuclear spin-contrast variation, a frozen sample plate containing paramagnetic impurities is required, for which the Cr(V)–EHBA complex ($Na[Cr(C_6H_{10}O_3)_2]\cdot H_2O$) was used, at a final concentration 0.85% (v/w). The matrix consisted of [$^{2}$H]glycerol (final concentration 54% (v/w)) and the sample

preparation procedure followed that described.[32] The final sample composition can be found in Table 2.

### Polarization-dependent small-angle neutron scattering

#### *General principles*

The scattering of thermal or cold neutrons by atoms in a sample is mainly due to the interaction between the incident neutron and the nucleus. The scattering is proportional to the scattering length, which varies with the isotope and its spin state. The most prominent examples are the scattering lengths for the two hydrogen isotopes: $^1$H (proton), $b_0 = -0.374 \times 10^{-12}$ cm and $^2$H (deuteron), $b_0 = +0.667 \times 10^{-12}$ cm. The difference in the scattering length density is called contrast. The contrast can be created or varied by isotopic substitution (substitution of $^1$H by $^2$H) either in the solvent (exchange of $H_2O$ by $^2H_2O$) or, if possible in the macromolecule itself. In the case of spin-contrast variation even the polarization-dependent change of the scattering length can be used. This is because the neutron, as well as the hydrogen nucleus, have a spin, resulting in scattering lengths that are dependent on the degree of polarization. A polarized neutron beam and a polarized $^1$H target have two possible relative spin orientations, viz. parallel ($\uparrow\uparrow$) or antiparallel ($\uparrow\downarrow$). The scattering lengths differ for these two possibilities: it is $+1.082 \times 10^{-12}$ cm when the spins are parallel ($\uparrow\uparrow$) or $-1.83 \times 10^{-12}$ cm when they are antiparallel ($\uparrow\downarrow$). Thus, the polarization-dependent scattering can vary over a wide range of different contrasts within one frozen sample. The other nuclei that are present in biological samples either show no changes in the scattering length with spin polarization (nuclear spin = 0), or are not affected by the polarization process (dynamic nuclear polarization, DNP) which is necessary to align the nuclear spins with respect to an external magnetic field.

Usually, isotopically labeled structures have the advantage that their biological activity is not severely influenced and thus can be considered as native particles. Ionization effects can be neglected and therefore radiation damage is not a problem with neutron scattering.

### Measurement and data treatment

In order to perform spin-contrast variation a frozen sample plate containing paramagnetic impurities is needed. We use the chromium(V)-EHBA complex (final concentration, 0.85% (v/w)). A matrix $d_8$-glycerol (final concentration, 54% (v/w)) in $^2H_2O$ was used. The sample preparation followed the procedure described[32] and the final sample composition can be found in Table 1. The data were collected at the small-angle scattering instrument SANS1 at the research reactor FRG1, GKSS research center[52] using the technique of DNP.[53,54]

The measurements for $^D$50 S-TF, $^D$70 S-TF and the respective solvents were performed as follows. The wavelength $\lambda$ was 8.5 Å with $\Delta\lambda/\lambda = 10\%$. The sample–detector distances were 0.7, 1.8 and 4.5 m, respectively, resulting in a $q$-range from 0.01 Å$^{-1}$ to 0.25 Å$^{-1}$ ($q$ is the scattering vector). All samples were measured in the unpolarized state ($P_H = P_D = 0$, one to two days) and as proton spin targets ($P_H \neq 0$, $P_D = 0$, three to four days) with parallel or antiparallel orientations of neutron and hydrogen spins. The measuring time for a single measurement was 1000 seconds resulting in about 300 measurements per sample over the entire five-day period of measurements. The proton polarization which could be obtained after DNPs were $P_H = -68\%$ for $^D$50 S-TF and $P_H = -62\%$ for $^D$70 S-TF. They decreased to $P_H = -60\%$ and $P_H = -58\%$, respectively, during the data collection. The solvent polarization was kept at $P_H = -78\%$ during the measurements.

The data treatment followed the procedures as described[33] resulting in a fitting routine for the basic scattering functions,[53] $U(q)^2$, Re$[U(q)V(q)]$ and $V(q)^2$, based on electron microscopy models. For the 50 S subunit a 40 Å resolution structure[37] and information about the protein distribution[55] were taken into account. The model calculations for 70 S exploited the 25 Å electron microscopy structure.[56] Even though higher resolution ribosomal structures are available, for example a 15 Å resolution structure,[57] a calculation of scattering curves with the 15 Å structure did not give a better representation of our measured ribosome data.

To determine the position of the label (e.g. of a protein) the scattering contributions of the three parts of the ribosome (RNA, total protein (TP) and label) to the scattering amplitudes $U$ and $V$ are calculated. While the scattering contributions of the RNA and TP are known, the scattering contribution of the label consisting of position and structure of the label is varied giving different scattering amplitudes for the label. From these scattering amplitudes the theoretical scattering intensity $I(q)_{calculated}$ is calculated and compared with the experimental scattering intensity $I(q)_{measured}$ using a least-squares fit routine to minimize the parameter $R$:

$$R = \left\{ \frac{1}{N} \sum_{i=1}^{N} \frac{(I(q)_{measured,i} - I(q)_{calculated,i})^2}{\sigma_i} \right\}^{1/2} = \text{Minimum}$$

for $N = 40$ intervals of $q$ in $0.01 < q < 0.2$ Å$^{-1}$ for all basic scattering functions. $\sigma_i$ is the standard deviation of the measured data. When the position of the label is searched first the coordinates represented in polar coordinates $R$, $\theta$ and $\varphi$ are varied in a step-width of 1–5 Å and 0.1–0.5 rad. When a minimum is reached the step-width becomes smaller, usually 0.1 Å and 0.01 rad. To check whether this is the best possible minimum and therefore an optimal position of the label with respect to the starting conditions, a minimum map is calculated. If this minimum map shows a better $R$-value the corresponding coordinates are used as starting parameters for the next fitting procedure.

## Acknowledgements

This work was supported by grants to K.H.N. from the Deutsche Forschungsgemeinschaft (grant Ni 174/8-3) and the Fonds der Chemischen Industrie. D.N.W. is grateful for support from the Alexander von Humboldt foundation.

## References

1. Hartl, U. (1996). Molecular chaperones in cellular protein folding. *Nature*, **381**, 571–580.

2. Bukau, B., Deuerling, E., Pfund, C. & Craig, E. A. (2000). Getting newly synthesized proteins into shape. *Cell*, **101**, 119–122.
3. Frydman, J. (2001). Folding of newly translated proteins *in vivo*: the role of molecular chaperones. *Annu. Rev. Biochem.* **70**, 603–647.
4. Crooke, E. & Wickner, W. (1987). Trigger factor: a soluble protein that folds pro-OmpA into a membrane-assembly-competent form. *Proc. Natl Acad. Sci. USA*, **84**, 5216–5220.
5. Crooke, E., Brundage, L., Rice, M. & Wickner, W. (1988). ProOmpA spontaneously folds in a membrane assembly competent state which trigger factor stabilizes. *EMBO J.* **7**, 1831–1835.
6. Crooke, E., Guthrie, B., Lecker, S., Lill, R. & Wickner, W. (1988). ProOmpA is stabilized for membrane translocation by either purified *E. coli* trigger factor or canine signal recognition particle. *Cell*, **54**, 1003–1011.
7. Guthrie, B. & Wickner, W. (1990). Trigger factor depletion or overproduction causes defective cell division but does not block protein export. *J. Bacteriol.* **172**, 5555–5562.
8. Stoller, G., Rucknagel, K. P., Nierhaus, K. H., Schmid, F. X., Fischer, G. & Rahfeld, J. U. (1995). A ribosome-associated peptidyl-prolyl *cis/trans* isomerase identified as the trigger factor. *EMBO J.* **14**, 4939–4948.
9. Valent, Q. A., Kendall, D. A., High, S., Kusters, R., Oudega, B. & Luirink, J. (1995). Early events in preprotein recognition in *E. coli*: interaction of SRP and trigger factor with nascent polypeptides. *EMBO J.* **14**, 5494–5505.
10. Hesterkamp, T., Hauser, S., Lutcke, H. & Bukau, B. (1996). *Escherichia coli* trigger factor is a prolyl isomerase that associates with nascent polypeptide chains. *Proc. Natl Acad. Sci. USA*, **93**, 4437–4441.
11. Zarnt, T., Tradler, T., Stoller, G., Scholz, C., Schmid, F. X. & Fischer, G. (1997). Modular structure of the trigger factor required for high activity in protein folding. *J. Mol. Biol.* **271**, 827–837.
12. Callebaut, I. & Mornon, J. P. (1995). Trigger factor, one of the *Escherichia coli* chaperone proteins, is an original member of the FKBP family. *FEBS Letters*, **374**, 211–215.
13. Hesterkamp, T. & Bukau, B. (1996). Identification of the prolyl isomerase domain of *Escherichia coli* trigger factor. *FEBS Letters*, **385**, 67–71.
14. Stoller, G., Tradler, T., Rucknagel, K. P., Rahfeld, J. U. & Fischer, G. (1996). An 11.8 kDa proteolytic fragment of the *E. coli* trigger factor represents the domain carrying the peptidyl-prolyl *cis/trans* isomerase activity. *FEBS Letters*, **384**, 117–122.
15. Lill, R., Crooke, E., Guthrie, B. & Wickner, W. (1988). The "trigger factor cycle" includes ribosomes, presecretory proteins, and the plasma membrane. *Cell*, **54**, 1013–1018.
16. Hesterkamp, T., Deuerling, E. & Bukau, B. (1997). The amino-terminal 118 amino acids of *Escherichia coli* trigger factor constitute a domain that is necessary and sufficient for binding to ribosomes. *J. Biol. Chem.* **272**, 21865–21871.
17. Patzelt, H., Rudiger, S., Brehmer, D., Kramer, G., Vorderwulbecke, S., Schaffitzel, E. *et al.* (2001). Binding specificity of *Escherichia coli* trigger factor. *Proc. Natl Acad. Sci. USA*, **98**, 14244–14249.
18. Scholz, C., Stoller, G., Zarnt, T., Fischer, G. & Schmid, F. X. (1997). Cooperation of enzymatic and chaperone functions of trigger factor in the catalysis of protein folding. *EMBO J.* **16**, 54–58.
19. Gothel, S. F., Scholz, C., Schmid, F. X. & Marahiel, M. A. (1998). Cyclophilin and trigger factor from *Bacillus subtilis* catalyze *in vitro* protein folding and are necessary for viability under starvation conditions. *Biochemistry*, **37**, 13392–13399.
20. Lyon, W. R., Gibson, C. M. & Caparon, M. G. (1998). A role for trigger factor and an rgg-like regulator in the transcription, secretion and processing of the cysteine proteinase of *Streptococcus pyogenes*. *EMBO J.* **17**, 6263–6275.
21. Huang, G. C., Li, Z. Y., Zhou, J. M. & Fischer, G. (2000). Assisted folding of D-glyceraldehyde-3-phosphate dehydrogenase by trigger factor. *Protein Sci.* **9**, 1254–1261.
22. Li, Z. Y., Liu, C. P., Zhu, L. Q., Jing, G. Z. & Zhou, J. M. (2001). The chaperone activity of trigger factor is distinct from its isomerase activity during co-expression with adenylate kinase in *Escherichia coli*. *FEBS Letters*, **506**, 108–112.
23. Kandror, O., Sherman, M., Rhode, M. & Goldberg, A. L. (1995). Trigger factor is involved in GroEL-dependent protein degradation in *Escherichia coli* and promotes binding of GroEL to unfolded proteins. *EMBO J.* **14**, 6021–6027.
24. Kandror, O., Sherman, M., Moerschell, R. & Goldberg, A. L. (1997). Trigger factor associates with GroEL *in vivo* and promotes its binding to certain polypeptides. *J. Biol. Chem.* **272**, 1730–1734.
25. Bukau, B. & Walker, G. C. (1989). Cellular defects caused by deletion of the *Escherichia coli* dnaK gene indicate roles for heat shock protein in normal metabolism. *J. Bacteriol.* **171**, 2337–2346.
26. Hesterkamp, T. & Bukau, B. (1998). Role of the DnaK and HscA homologs of Hsp70 chaperones in protein folding in *E. coli*. *EMBO J.* **17**, 4818–4828.
27. Deuerling, E., Schulze-Specking, A., Tomoyasu, T., Mogk, A. & Bukau, B. (1999). Trigger factor and DnaK cooperate in folding of newly synthesized proteins. *Nature*, **400**, 693–696.
28. Teter, S. A., Houry, W. A., Ang, D., Tradler, T., Rockabrand, D., Fischer, G. *et al.* (1999). Polypeptide flux through bacterial Hsp70: DnaK cooperates with trigger factor in chaperoning nascent chains. *Cell*, **97**, 755–765.
29. Bang, H., Pecht, A., Raddatz, G., Scior, T., Solbach, W., Brune, K. & Pahl, A. (2000). Prolyl isomerases in a minimal cell. Catalysis of protein folding by trigger factor from *Mycoplasma genitalium*. *Eur. J. Biochem.* **267**, 3270–3280.
30. Capel, M. S., Engelman, D. M., Freeborn, B. R., Kjeldgaard, M., Langer, J. A., Ramakrishnan, V. *et al.* (1987). A complete mapping of the proteins in the small ribosomal subunit of *Escherichia coli*. *Science*, **238**, 1403–1406.
31. May, R. P., Nowotny, V., Nowotny, P., Voss, H. & Nierhaus, K. H. (1992). Inter-protein distances within the large subunit from *Escherichia coli* ribosomes. *EMBO J.* **11**, 373–378.
32. Willumeit, R., Burkhardt, N., Diedrich, G., Zhao, J., Nierhaus, K. H. & Stuhrmann, H. B. (1996). The *in situ* structure of ribosomal proteins from polarized neutron scattering. *J. Mol. Struct.* **383**, 201–211.
33. Willumeit, R., Burkhardt, N., Wadzack, J., Nierhaus, K. H. & Stuhrmann, H. B. (1997). Localisation of proteins and tRNA molecules in the 70 S ribosome of the *E. coli* bacteria with polarized neutron scattering. *J. Appl. Crystallog.* **30**, 1125–1131.
34. Jünemann, R., Burkhardt, N., Wadzack, J., Schmitt, M., Willumeit, R., Stuhrmann, H. B. & Nierhaus,

K. H. (1998). Small angle scattering in ribosomal structure research: localisation of the messenger RNA within the ribosomal elongation states. *Biol. Chem.* **379**, 807–818.
35. Nierhaus, K. H., Wadzack, J., Burkhardt, N., Jünemann, R., Meerwinck, W., Willumeit, R. & Stuhrmann, H. B. (1998). Structure of the elongating ribosome: arrangement of the two tRNAs before and after translocation. *Proc. Natl Acad. Sci. USA*, **95**, 945–950.
36. Svergun, D. I. & Nierhaus, K. H. (2000). A map of protein–rRNA distribution in the 70 S *Escherichia coli* ribosome. *J. Biol. Chem.* **275**, 14432–14439.
37. Frank, J., Penczek, P., Grassucci, R. & Srivastava, S. (1991). Three dimensional reconstruction of the 70 S *Escherichia coli* ribosome in ice: the distribution of ribosomal RNA. *J. Cell Biol.* **115**, 597–605.
38. Frank, J., Verschoor, A., Li, Y. H., Zhu, J., Lata, R. K., Radermacher, M. *et al.* (1995). A model of the translational apparatus based on a three-dimensional reconstruction of the *Escherichia coli* ribosome. *Biochem. Cell Biol.* **73**, 757–765.
39. Blaha, G., Burkhardt, N. & Nierhaus, K. H. (2002). Formation of 70 S ribosomes: large activation energy is required for the adaptation of exclusively the small ribosomal subunit. *Biophys. Chem.* **96**, 153–161.
40. Malkin, L. I. & Rich, A. (1967). Partial resistance of nascent polypeptide chains to proteolytic digestion due to ribosomal shielding. *J. Mol. Biol.* **26**, 329–346.
41. Blobel, G. & Sabatini, D. D. (1970). Controlled proteolysis of nascent polypeptides in rat liver cell fractions. I. Location of the polypeptides within ribosomes. *J. Cell Biol.* **45**, 130–145.
42. Smith, W. P., Tai, P. C. & Davis, B. D. (1978). Nascent peptide as sole attachment of polysomes to membranes in bacteria. *Proc. Natl Acad. Sci. USA*, **75**, 814–817.
43. Lim, V. I. & Spirin, A. S. (1986). Stereochemical analysis of ribosomal transpeptidation. Conformation of nascent peptide. *J. Mol. Biol.* **188**, 565–574.
44. Lim, V. I. & Spirin, A. S. (1985). Stereochemistry of the transpeptidation reaction in the ribosome. The ribosome generates an alpha-helix in the synthesis of the polypeptide chain. *Dokl. Akad. Nauk SSSR*, **280**, 235–239.
45. Ban, N., Nissen, P., Hansen, J., Moore, P. B. & Steitz, T. A. (2000). The complete atomic structure of the large ribosomal subunit at 2.4 Å resolution. *Science*, **289**, 905–920.
46. Harms, J., Schluenzen, F., Zarivach, R., Bashan, A., Gat, S., Agmon, I. *et al.* (2001). High resolution structure of the large ribosomal subunit from a mesophilic eubacterium. *Cell*, **107**, 679–688.
47. Kramer, G., Rauch, T., Rist, W., Vorderwülbecke, S., Patzelt, H., Schulze-Specking, A. *et al.* (2002). L23 protein functions as a chaperone docking site on the ribosome. *Nature*, **419**, 171–174.
48. Pool, M. R., Stumm, J., Fulga, T. A., Sinning, I. & Dobberstein, B. (2002). Distinct modes of signal recognition particle interaction with the ribosome. *Science*, **291**, 1345–1348.
49. Albanese, V. & Frydman, J. (2002). Where chaperones and nascent polypeptides meet. *Nature Struct. Biol.* **9**, 716–718.
50. Vanatalu, K., Paalme, T., Vilu, R., Burkhardt, N., Jünemann, R., May, R. *et al.* (1993). Large-scale preparation of fully deuterated cell components. Ribosomes from *Escherichia coli* with high biological activity. *Eur. J. Biochem.* **216**, 315–321.
51. Rheinberger, H.-J., Geigenmüller, U., Wedde, M. & Nierhaus, K. H. (1988). Parameters important for the preparation of *E. coli* ribosomes and ribosomal subunits highly active in tRNA binding. *Methods Enzymol.* **164**, 658–670.
52. Zhao, J., Meerwinck, W., Niinikoski, T., Rijllart, A., Schmitt, M. & Willumeit, R. (1995). The polarized target station at GKSS. *Nucl. Instrum. Methods Phys. Res.* A**356**, 133–137.
53. Abragam, A. & Goldman, M. (1992). *Nuclear Magnetism, Order and Disorder*, Clarendon Press, Oxford.
54. Borghini, M. (1972). Mechanism of nuclear dynamic polarisation by electron-nucleus dipole coupling in solids. In *Proceedings of the Second International Conference on Polarized Targets* (Shapiro, G., ed.), National Technical Information Service, Springfield, VA.
55. Walleczek, J., Schuler, D., Stöffler-Meilicke, M., Brimacombe, R. & Stöffler, G. (1988). A model for the spatial arrangement of the proteins in the large subunit of the *Escherichia coli* ribosome. *EMBO J.* **7**, 3571–3576.
56. Frank, J., Zhu, J., Penczek, P., Li, Y. H., Srivastava, S., Verschoor, A. *et al.* (1995). A model of protein synthesis based on cryo-electron microscopy of the *E. coli* ribosome. *Nature*, **376**, 441–444.
57. Malhotra, A., Penczek, P., Agrawal, R. K., Gabashvili, I. S., Grassucci, R. A., Jünemann, R. *et al.* (1998). *E. coli* 70 S ribosome at 15 Å resolution by cryo-electron microscopy: localization of fMet-tRNA$_f^{Met}$ and fitting of L1 protein. *J. Mol. Biol.* **280**, 103–116.

***Edited by J. Doudna***

*(Received 13 June 2002; received in revised form 6 November 2002; accepted 8 December 2002)*